Inorganic Chemistry

· Article

The Structure of ([W₃Q₄X₃(dmpe)₃]⁺, Y⁻) Ion Pairs (Q = S, Se; X = H, OH, Br; Y = BF₄, PF₆, dmpe = Me₂PCH₂CH₂PMe₂) in Dichloromethane Solution and the Effect of Ion-Pairing on the Kinetics of Proton Transfer to the Hydride Cluster [W₃S₄H₃(dmpe)₃]⁺

Andrés G. Algarra,[†] Manuel G. Basallote,*,[†] M. Jesús Fernández-Trujillo,[†] Rosa Llusar,*,[‡] Vicent S. Safont,[‡] and Cristian Vicent[‡]

Departamento de Ciencia de los Materiales e Ingeniería Metalúrgica y Química Inorgánica, Facultad de Ciencias, Universidad de Cádiz, Apartado 40, Puerto Real, 11510 Cádiz, Spain, and Departament de Ciències Experimentals, Universitat Jaume I, Campus de Riu Sec, P.O. Box 224, Castelló, Spain

The ¹H,¹⁹F HOESY spectra of the title compounds in CD₂Cl₂ solution indicate that the cluster cations form ion pairs with the BF₄⁻ and PF₆⁻ anions with a well-defined interionic structure that appears to be basically determined essentially by the nature of the X⁻ ligand. For the clusters with X = H and OH, the structure of the ion pairs is such that the counteranion (Y⁻) and the X⁻ ligands are placed close to each other. However, when the size and electron density of X⁻ increase (X = Br), Y⁻ is forced to move to a different site, far away from X⁻. The relevance of ion-pairing on the chemistry of these compounds is clearly seen through a decrease in the rate of proton transfer from HCl to the hydride cluster [W₃S₄H₃(dmpe)₃]⁺ in the presence of an excess of BF₄⁻. The kinetic data for this reaction can be rationalized by considering that the ([W₃S₄H₃(dmpe)₃]⁺, BF₄⁻) ion pairs are unproductive in the proton-transfer process. Theoretical calculations indicate that the real behavior can be more complex. Although the cluster can still form adducts with HCl in the presence of BF₄⁻, the structures of the most-stable BF₄⁻-containing HCl adducts show H···H distances too large to allow the subsequent release of H₂. In addition, the effective concentration of HCl is also reduced because of the formation of adducts as ClH···BF₄⁻. As a consequence of both effects, the proton transfer takes place more slowly than for the case of the dihydrogen-bonded HCl adduct resulting from the unpaired cluster.

Introduction

In nonaqueous solvents of low dielectric constants, the electrostatic interactions between cations and anions are significantly stronger than in water, which favors the formation of ion pairs and higher aggregates. As a consequence, ionic complexes do not usually exist in those solvents as simply solvated species but as ion pairs, which may lead to different reactivity patterns depending on the nature of the counterion.[1] Ion-pairing can affect both the thermodynamics of a reaction, by changing the relative energies of the reagents and the products, and its kinetics and mecha-

nism, by providing alternative reaction pathways.[2] For this reason, there is nowadays a growing interest aimed at elucidating the structure of transition-metal complexes in solution. Very useful NMR procedures have been developed for this purpose, with special emphasis on the interaction between cationic complexes and fluorine-containing anions.[3] The experimental NMR procedures developed for the study

* To whom correspondence should be addressed. E-mail: llusar@exp.uji.es (R.L.); manuel.basallote@uca.es (M.G.B.).
† Universidad de Cádiz.
‡ Universitat Jaume I.

(1) (a) Trost, B. M.; Bunt, R. C. *J. Am. Chem. Soc.* **1998**, *120*, 70. (b) Kovacevic, A.; Gründemann, S.; Miecznikowski, J. R.; Clot, E.; Eisenstein, O.; Crabtree, R. H. *Chem. Commun.* **2003**, 2580. (c) Gruet, K.; Clot, E.; Eisenstein, O.; Lee, D. H.; Patel, B.; Macchioni, A.; Crabtree, R. H. *New J. Chem.* **2003**, *27*, 80.
(2) (a) Romeo, R.; Arena, R.; Scolaro, L. M.; Plutino, R. M. *Inorg. Chim. Acta* **1995**, *241*, 81. (b) Kovacevic, A.; Gründemann, S.; Miecznikowski, J. R.; Clot, E.; Eisenstein, O.; Crabtree, R. H. *Chem. Commun.* **2002**, 2580. (c) Barge, A.; Botta, M.; Parker, D.; Puschmann, H. *Chem. Commun.* **2003**, 1386. (d) Aullón, G.; Esquius, G.; Lledós, A.; Maseras, F.; Pons, J.; Ros, J. *Organometallics* **2004**, *23*, 5530.

of these interactions and the relevance of ion-pairing in inorganic and organometallic chemistry have been discussed in two recent reviews.[4] As a summary, it can be stated that the information available to date indicates that anions do not necessarily approach the metal complex at sites where the distance to the metal center is minimized; instead, other unexpected sites are often preferred. These observations support the idea of an asymmetric distribution of the positive charge in cationic metal complexes, which can no longer be considered as being the positively charged spheres assumed in classical treatments on the formation of outer-sphere complexes.[5]

On the other hand, cubane type clusters with metal centers bridged by sulfides or selenides are a topic of current interest because of their relevance to metalloenzymes and industrial catalysis[6] together with their applications in fields such as nonlinear optics[7,8] and medicine.[9] For the past few years, we have been studying the chemistry of incomplete cuboidal clusters of formula $[M_3Q_4X_3(\text{diphosphine})_3]^+$ (M = Mo, W; Q = S, Se; X = H, OH, Cl, Br; diphosphine = dmpe, dppe), focusing our attention not only on their synthetic, structural, and theoretical aspects[10] but also on their applications and elucidation of the mechanisms of some of their relevant reactions.[11−13] During these investigations, we realized that

Chart 1

Cluster	Q	X
1⁺	S	H
2⁺	S	OH
3⁺	S	Br
4⁺	Se	H
5⁺	Se	OH
6⁺	Se	Br
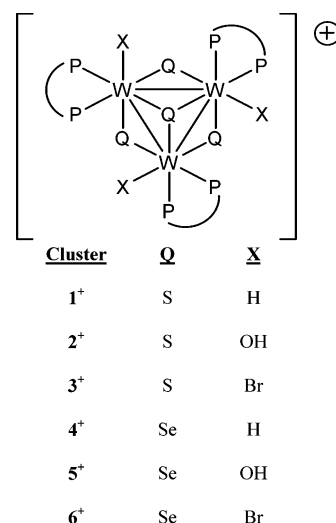
a deeper understanding on the reactivity of these compounds could be achieved through a better knowledge of the structure of the ion pairs formed in solution by these M_3Q_4 cluster cations. The single positive charge in $[W_3Q_4X_3(\text{diphosphine})_3]^+$ may be delocalized over the whole trinuclear cluster, and several sites of interaction with the anion are possible. Anion interaction at specific cluster sites could provide relevant information regarding the preferred approach position by an external reagent. For this reason, this work focuses on the interactions between the complexes $[W_3Q_4X_3(\text{diphosphine})_3]^+$ (Q = S, Se; X = H, OH, Br) and two different fluorinated counterions, namely BF_4^- and PF_6^-. These anions have been selected not only because of their inert character (as a matter of fact, their salts are often used to control the ionic strength in kinetic experiments involving charged reagents) but also because of their potential as probes for detecting specific interactions by NMR techniques. Chart 1 summarizes the complexes investigated and their numbering scheme.

A reaction in which ion-pair formation may become particularly important is the proton transfer from acids to metal-coordinated hydrides. The interaction between M−H and H−X fragments leads initially to the formation of an M−H•••H−X dihydrogen bond that can evolve to a dihydrogen complex depending on the acid−base properties of the reagents.[14] Proton-transfer mechanism elucidation is essential for understanding heterolytic activation of H_2 and catalytic hydrogenations,[15] and the trinuclear $[W_3S_4H_3(\text{dmpe})_3]^+$ hydride (**1⁺**) has revealed very useful information in this regard.[12,13] Thus, the reaction of **1⁺** with an excess of HCl and other acids in dichloromethane solution occurs with

(3) (a) Bellachioma, G.; Cardaci, G.; Macchioni, A.; Reichenbach, G.; Terenzi, S. *Organometallics* **1996**, *15*, 4349. (b) Macchioni, A.; Bellachioma, G.; Cardaci, G.; Gramlich, H.; Rüeger, H.; Terenzi, S. *Organometallics* **1997**, *16*, 2139. (c) Hofstetter, C.; Pochapsky, T. C. *Magn. Reson. Chem.* **2000**, *38*, 90. (d) Macchioni, A.; Zuccaccia, C.; Clot, E.; Gruet, K.; Crabtree, R. H. *Organometallics* **2001**, *20*, 2367. (e) Zuccaccia, C.; Bellachioma, G.; Cardaci, G.; Macchioni, A. *J. Am. Chem. Soc.* **2001**, *123*, 11020. (f) Drago, D.; Pregosin, P. S.; Pfaltz, A. *Chem. Commun.* **2002**, 286. (g) Macchioni, A. *Eur. J. Inorg. Chem.* **2003**, 195. (h) Kumar, P. G. A.; Pregosin, P. S.; Goicoechea, J. M.; Whittlesey, M. K. *Organometallics* **2003**, *22*, 2956. (i) Martínez-Viviente, E.; Pregosin, P. S. *Inorg. Chem.* **2003**, *42*, 2209. (j) Pregosin, P. S.; Martínez-Viviente, E.; Kumar, P. G. A. *Dalton Trans.* **2003**, 4007. (k) Zuccaccia, D.; Sabatini, S.; Bellachioma, G.; Cardaci, G.; Clot, E.; Macchioni, A. *Inorg. Chem.* **2003**, *42*, 5465. (l) Zuccaccia, D.; Stahl, N. G.; Macchioni, A.; Chen, M. C.; Roberts, J. A.; Marks, T. J. *J. Am. Chem. Soc.* **2004**, *126*, 1448. (m) Schott, D.; Pregosin, P. S.; Veiros, L. F.; Calhorda, M. J. *Organometallics* **2005**, *24*, 5710. (n) Appelhans, L. N.; Zuccaccia, D.; Kovacevic, A.; Chianese, A. R.; Miecznikowski, J. R.; Macchioni, A.; Clot, E.; Eisenstein, O.; Crabtree, R. H. *J. Am. Chem. Soc.* **2005**, 127, 16299.

(4) (a) Macchioni, A. *Chem. Rev.* **2005**, 105, 2039. (b) Pregosin, P. S.; Anil Kumar, P. G.; Fernández, I. *Chem. Rev.* **2005**, *105*, 2977.

(5) Probably the most-popular treatment of this type is that of Fuoss (Fuoss, R. M. *J. Am. Chem. Soc.* **1958**, *80*, 5059), which is frequently used to estimate the equilibrium constant for the formation of the outer-sphere complex in substitution reactions occurring through an Eigen−Wilkins mechanism.

(6) Stiefel, E. I.; Matsumoto, K. *Transition Metal Sulfur Chemistry*; ACS Symposium Series 653; American Chemical Society: Washington, DC, 1995.

(7) (a) Hou, H. W.; Xin, X. Q.; Shi, S. C*oord. Chem. Rev.* **1996**, *153*, 25. (b) Zhang, C.; Song, Y. L.; Wang, X.; Kuhn, F. E.; Wang, Y. X.; Xu, Y.; Xin, X. Q. *J. Mater. Chem.* **2003**, *13*, 571.

(8) Feliz, M.; Garriga, J. M.; Llusar, R.; Uriel, S.; Humphrey, M. G.; Lucas, N. T.; Samoc, M.; Luther-Davies, B. *Inorg. Chem.* **2001**, *40*, 6132.

(9) (a) Yu, S. B.; Watson, A. D. *Chem. Rev.* **1999**, *99*, 2353. (b) Yu, S. B.; Droege, M.; Segal, B.; Kim, S. H.; Sanderson, T.; Watson, A. D. *Inorg. Chem.* **2000**, *39*, 1325.

(10) (a) Feliz, M.; Llusar, R.; Andrés, J.; Beski, S.; Silvi, B. *New J. Chem.* **2002**, *26*, 844. (b) Llusar, R.; Uriel, S. *Eur. J. Inorg. Chem.* **2003**, 1271. (c) Feliz, M.; Llusar, R.; Uriel, S.; Vicent, C.; Coronado, C.; Gómez-García, C. J. *Chem. Eur. J.* **2004**, *10*, 4308.

(11) Basallote, M. G.; Estevan, F.; Feliz, M.; Fernández-Trujillo, M. J.; Hoyos, D. A.; Llusar, R.; Uriel, S.; Vicent, C. *J. Chem. Soc., Dalton Trans.* **2004**, 530.

(12) Basallote, M. G.; Feliz, M.; Fernández-Trujillo, M. J.; Llusar, R.; Safont, V. S.; Uriel, S. *Chem.—Eur. J.* **2004**, *10*, 1463.

(13) Algarra, A. G.; Basallote, M. G.; Feliz, M.; Fernández-Trujillo, M. J.; Llusar, R.; Safont, V. S. *Chem. Eur. J.* **2006**, *13*, 1413.

(14) (a) Jessop, P. G.; Morris, R. H. *Coord. Chem. Rev.* **1992**, *121*, 155. (b) Heinekey, D. M.; Oldham, W. J. *Chem. Rev.* **1993**, *93*, 913. (c) Basallote, M. G.; Durán, J.; Fernández-Trujillo, M. J.; Máñez, M.; Rodríguez de la Torre, J. *J. Chem. Soc., Dalton Trans.* **1998**, 745. (d) Peruzzini, M.; Poli, R., Eds.; *Recent Advances in Hydride Chemistry*; Elsevier: Amsterdam, 2001. (e) Kubas, G. J. *Metal Dihydrogen and σ-Bond Complexes: Structure, Theory and Reactivity*; Kluwer: New York, 2001. (f) Bakhmutov, V. I. *Eur. J. Inorg. Chem.* **2005**, 245.

Table 1. Chemical Shifts for the Signals Observed in the $^{31}P\{^1H\}$ and ^1H NMR Spectra of Clusters 1^+-6^+ in CD$_2$Cl$_2$ Solution

	phosphorus signals[a]		proton signals[a]				
cluster	P(1)[b]	P(2)	Me(6)	Me(5)	Me(1)	Me(2)	other
1	11.8	−7.6	0.45	1.70	2.15	2.38	−0.92[c]
2	10.6	−5.1	0.65	1.57	1.89	2.17	3.40[d]
3	1.2	−1.4	0.95	1.82	2.24	2.42	
4	15.9	−11.2	0.57	1.87	2.30	2.55	−2.45[c]
5	13.8	−7.2	0.62	1.55	1.85	2.32	3.75[d]
6	7.9	−2.3	0.96	1.89	2.50	2.51	

[a] See Figure 1 for the nomenclature of the phosphorus and methyl signals. [a] The spectra obtained for the BF$_4^-$ and PF$_6^-$ salts do not show any significant difference. The positions of the protons in the ethylenic chain of the dmpe ligand have been omitted for simplicity. [b] Phosphorus trans to μ_3-Q^{2-}. [c] Hydride signal. [d] OH signal.

a second-order dependence with respect to the acid that can be rationalized in terms of the formation of W−H···H−Cl···H−Cl adducts, which evolve into the chloro complex with H$_2$ release.[13] The reaction occurs through a transition state that can be described as a dihydrogen complex ion-paired to HCl$_2^-$. As ion-pairing with BF$_4^-$ has recently been shown to provide an efficient pathway for the proton transfer from the dihydrogen complex *trans*-[FeH(H$_2$)(dppe)$_2$]$^+$ to a base,[16] we wondered how the ([W$_3$S$_4$H$_3$(dmpe)$_3$]$^+$, BF$_4^-$) ion-pair formation could affect the kinetics and mechanism of proton transfer in this case. The results of both kinetic experiments and theoretical calculations are also included in the paper.

Results and Discussion

NMR Studies on the Interaction of the [W$_3$Q$_4$X$_3$dmpe$_3$]$^+$ Clusters with PF$_6^-$ and BF$_4^-$ in CD$_2$Cl$_2$ Solution. The ^1H and $^{31}P\{^1H\}$ NMR spectra of the BF$_4^-$ and PF$_6^-$ salts of the cationic clusters 1^+-6^+ recorded in CD$_2$Cl$_2$ solution (Table 1) are similar to those previously reported for salts with other anions.[11,12,17−19] The $^{31}P\{^1H\}$ spectra show the AX pattern expected for two nonequivalent phosphorus nuclei but the small $^2J_{P-P}$ values usually result in the appearance of two singlets with the characteristic satellite peaks caused by coupling to the ^{183}W nuclei. The ^1H spectra show four resonances for the methyl protons, which appear as doublets with $^2J_{H-P} = 9-11$ Hz, and four strongly coupled resonances
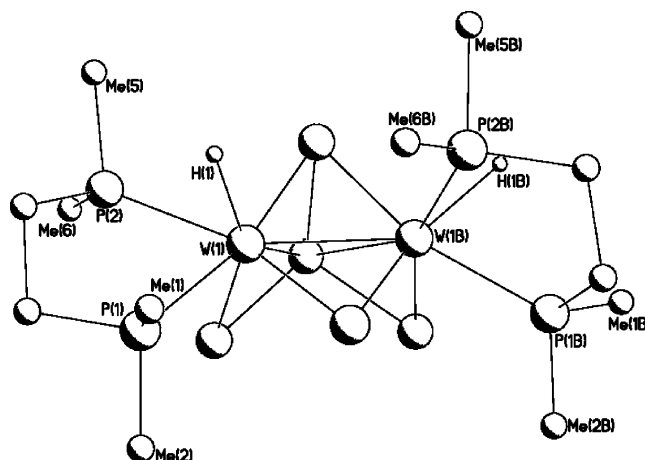
(15) (a) Esteruelas, M. A.; Oro, L. A. *Chem. Rev.* **1998**, *98*, 577. (b) Bullock, R. M.; Voges, M. H. *J. Am. Chem. Soc.* **2000**, *122*, 12594. (c) Rautenstrauch, V.; Hoang-Cong, X.; Churlaud, R.; Abdur-Rashid, K.; Morris, R. H. *Chem.—Eur. J.* **2003**, *9*, 4954. (d) Clapham, S. E.; Hadzovic, A.; Morris, R. H. *Coord. Chem. Rev.* **2004**, *248*, 2201. (e) Justice, A. K.; Linck, R. C.; Rauchfuss, T. B.; Wilson, S. R. *J. Am. Chem. Soc.* **2004**, *126*, 13214. (f) Bullock, R. M. *Chem.—Eur. J.* **2004**, *10*, 2366. (g) Abbel, R.; Abdur-Rashid, K.; Faatz, M.; Hadzovic, A.; Lough, A. J.; Morrris, R. H. *J. Am. Chem. Soc.* **2005**, *127*, 1870. (h) Casey, C. P.; Johnson, J. B. *J. Am. Chem. Soc.* **2005**, *127*, 1883. (i) Hamilton, R. J.; Leong, C. G.; Bigam, G.; Miskolzie, M.; Bergens, S. H. *J. Am. Chem. Soc.* **2005**, *127*, 4152. (j) Lamle, S. E.; Albracht, S. P. J.; Armstrong, F. A. *J. Am. Chem. Soc.* **2005**, *127*, 6595. (k) Guan, H.; Iimura, M.; Magee, M. P.; Norton, J. R.; Zhu, G. *J. Am. Chem. Soc.* **2005**, *127*, 7805.
(16) Basallote, M. G.; Besora, M.; Durán, J.; Fernández-Trujillo, M. J.; Lledós, A.; Máñez, M. A.; Maseras, F. *J. Am. Chem. Soc.* **2004**, *126*, 2320.
(17) Llusar, R.; Uriel, S.; Vicent, C. *J. Chem. Soc., Dalton Trans.* **2001**, 2813.
(18) Cotton, F. A.; Mandal, S. K. *Inorg. Chim. Acta* **1992**, *192*, 71.
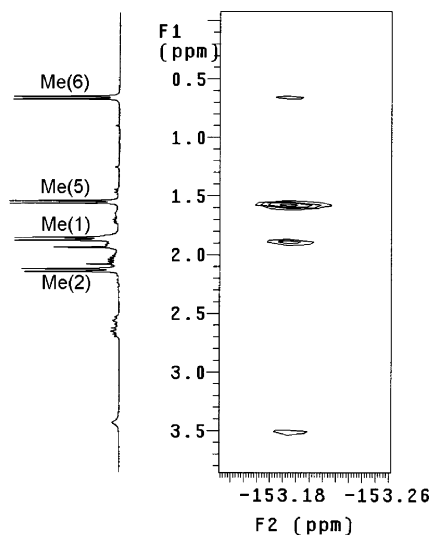(19) Cotton, F. A.; Llusar, R.; Eagle, C. T. *J. Am. Chem. Soc.* **1989**, *111*, 4332.

Figure 1. Structure of cluster 1^+ showing the notation used in this work for the different NMR signals. The environment on one metal site has been omitted for clarity.

that correspond to the diastereotopic hydrogen atoms of the ethylene bridge of the phosphine. The hydride signal in clusters 1^+ and 4^+ appears as a doublet of doublets because of the coupling with the nonequivalent phosphorus atoms, and the signal for the hydroxyl proton appears as a broad singlet in the spectra of complexes 2^+ and 5^+. On the basis of the results obtained with selective phosphorus decoupling and NOESY1D NMR experiments (see the Supporting Information), we could assign the signals to the different unequivalent phosphorus and methyl groups, and the results are also included in Table 1 using the notation in Figure 1.

The interionic structure of the PF$_6^-$ and BF$_4^-$ salts of clusters 1^+-6^+ was then investigated by recording their $^1H,^{19}F$ HOESY spectra in CD$_2$Cl$_2$ solution. Dipolar interactions between the protons of the cluster methyl groups and the fluorine nuclei of the anion are observed in all cases. The potential contacts between the anion fluorine nuclei and the protons in the ethylene group are significantly weaker; although some weak signals could be detected when looking at the internal ^1H projections in some of the HOESY spectra, the signal-to-noise ratio is not large enough to obtain reliable measurements. For hydroxo complex 2^+, a significant interaction was seen between the BF$_4^-$ anion and the hydroxyl ligands (see Figure 2) that was not observed in any other system. In this case, the proton of the OH group bears a partial positive charge that favors the interaction with the negatively charged BF$_4^-$ anion. The absence of such a signal for the other hydroxo complex studied (5^+) is probably due to the lower signal-to-noise ratio in the spectrum. No interionic contacts were observed between the anions and the hydride ligands in clusters 1^+ and 4^+.

Because of the special arrangement of the methyl groups in the incomplete cuboidal structure, the contacts between the protons in the cationic cluster and the fluorines in the anion provide very useful information for determining the anion-preferred sites of approach and the interionic structure in solution. The signals observed in the HOESY spectra of the BF$_4^-$ and PF$_6^-$ salts of clusters 1^+-6^+ are summarized in Table 2 with the intensities normalized through the factor $[n_I n_S/(n_I + n_S)]$, where n_I and n_S stand for the number of

Figure 2. ^{1}H,^{19}F HOESY spectrum of [W$_3$S$_4$(OH)$_3$(dmpe)$_3$](BF$_4$) in CD$_2$-Cl$_2$ solution.

Table 2. Intensity of the Cross-Peaks Observed in the ^{1}H,^{19}F HOESY Spectra of the Salts of Clusters **1**$^+$−**6**$^+$ in CD$_2$Cl$_2$ Solution

		proton signals and normalized NOE intensities				
cluster	anion	Me(6)	Me(5)	Me(1)	Me(2)	OH
1$^+$	BF$_4$$^-$	0.50	1.00	0.94		
1$^+$	PF$_6$$^-$	0.89	1.00	0.84		
2$^+$	BF$_4$$^-$	0.18	1.00	0.34		0.29
2$^+$	PF$_6$$^-$	0.43	1.00	0.46	0.17	
3$^+$	BF$_4$$^-$	0.36		1.00	0.57	
3$^+$	PF$_6$$^-$	0.25		1.00	0.59	
4$^+$	BF$_4$$^-$	0.13	1.00	0.22		
4$^+$	PF$_6$$^-$	0.20	1.00	0.52		
5$^+$	BF$_4$$^-$	0.28	1.00	0.31		
5$^+$	PF$_6$$^-$		1.00	0.46		
6$^+$	BF$_4$$^-$	0.35	0.49	1.00^a	1.00^a	
6$^+$	PF$_6$$^-$			1.00^a	1.00^a	

^{a} The measurement of separate intensities is hindered by the overlapping of the Me(1) and Me(2) signals.

equivalent nuclei of both types (^{1}H and ^{19}F),[20] and then scaled by arbitrarily fixing to 1 the most-intense contact in each spectrum.

From the whole set of spectra, it can be established that there is a unique preferred interionic structure for each cluster−anion combination, although the interionic structure of the hydride and hydroxo clusters (X = H, OH) differs from that of the bromide complexes (X = Br). Thus, for the **1**$^+$, **2**$^+$, **4**$^+$, and **5**$^+$ cations, the strongest contact corresponds to the interaction between the fluorine atoms of the anion and the Me(5) protons. There is also a signal for the fluorine nuclei interaction with the Me(1) protons and a weaker contact with Me(6) (see Figure 2). In only one case ([**2**]-PF$_6$), a very weak signal for the interaction with Me(2) is observed. These results can be interpreted on the basis of the interionic structure shown in Figure 3a. In this figure, the cluster is represented with the W$_3$ triangle defining a plane that divides the cation in two parts. The μ_3-Q, X, and P(2) atoms are placed above this plane, whereas P(1) and the μ_2-Q ligands are located below it. The methyl groups Me(5) and Me(2) are roughly perpendicular to the metal
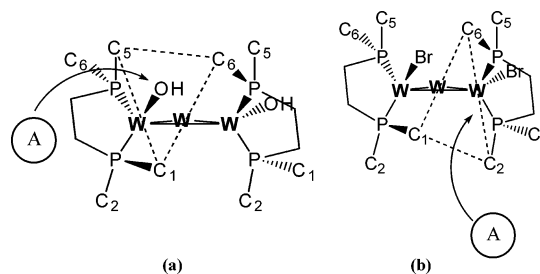
(20) Macura, S.; Ernst, R. R. *Mol. Phys.* **1980**, *41*, 95.

Figure 3. Proposed interionic structure in CD$_2$Cl$_2$ solution for the ion pairs formed by the [W$_3$Q$_4$X$_3$(dmpe)$_3$]$^+$ clusters with the BF$_4$$^-$ and PF$_6$$^-$ anions. The anion is represented by A, and the figure is particularized for cluster **2**$^+$. Drawing (a) corresponds to the ion pairs formed by clusters **1**$^+$, **2**$^+$, **4**$^+$, and **5**$^+$, whereas (b) represents the preferred site of approach of the anions to the **3**$^+$ and **6**$^+$ clusters.
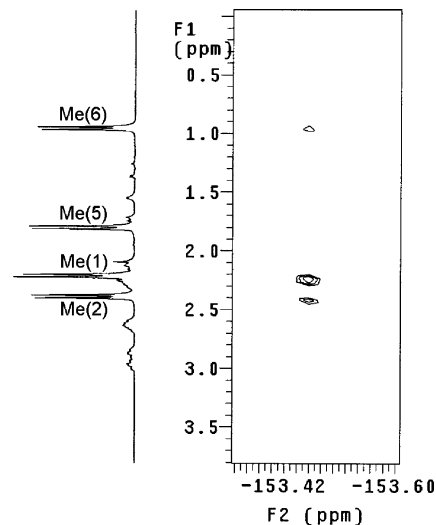

Figure 4. ^{1}H,^{19}F HOESY spectrum of [W$_3$S$_4$Br$_3$(dmpe)$_3$](BF$_4$) in CD$_2$-Cl$_2$ solution.

plane but directed upward and downward, respectively. In contrast, Me(6) and Me(1) are roughly parallel to the plane but point toward opposite directions. The site of approach of the BF$_4$$^-$ and PF$_6$$^-$ anions is that defined by the Me(5), Me(1), and Me(6) triangle, depicted in Figure 3a, although the relative intensities of the HOESY signals show that the preferential site of approach within the triangle occurs closer to the Me(5)−Me(1) edge and the Me(5) vertex. Although only one triangle has been represented in Figure 3, there are actually three equivalent sites imposed by the C_3 symmetry of the cluster. The contact observed between the BF$_4$$^-$ anion and the OH group in cluster **2**$^+$ supports the above interpretation, where the anion approaches the upper side of the W$_3$ triangle; however, replacement of BF$_4$$^-$ by the larger PF$_6$$^-$ anion or substitution of the OH group by the hydride ligand result in the absence of interaction between the external anion and the X$^-$ ligand, which indicates that small changes in the cluster or anion sizes may determine the observation or the absence of X$^-$−anion interactions in the spectra.

The HOESY spectra for the salts of the bromine complexes **3**$^+$ and **6**$^+$ (see Figure 4) suggest a structure for the ion pair that is different from the one just described for the hydride and hydroxo complexes. For cluster **3**$^+$, the intensities of the contacts indicate that the anion approaches the cluster

pointing toward the triangle defined by the Me(1), Me(2), and Me(6) methyl groups (see Figure 3b) and having the Me(1)−Me(2) edge and the Me(1) vertex as preferential positions. In consequence, substitution of the H$^-$ or OH$^-$ ligands by the larger and more-electron-rich Br$^-$ anion results in a change in the interionic structure, in such a way that the anion moves away from the X$^-$ ligand and approaches the metal triangle from the bottom side. For the other bromo complex, Se cluster 6^+, the structure of the ion pair formed with the PF$_6^-$ anion is roughly the same as the one found for the analogous S compound (Figure 3b); however, the intensities of the contacts for the pair 6^+−BF$_4^-$ suggest that the anion approaches the cluster cation on both sides of the W$_3$ triangle (*a* and *b* in Figure 3); i.e., the small increase in the cluster size upon replacement of S by Se seems to be enough to allow the accommodation of the smaller BF$_4^-$ anion at positions close to the bromide ligand.

These results demonstrate that the [W$_3$Q$_4$X$_3$(dmpe)$_3$]$^+$ clusters form in CD$_2$Cl$_2$ solution ion pairs of well-defined interionic structure with the BF$_4^-$ and PF$_6^-$ anions. The interionic structure in solution appears to be mainly determined by minimization of the repulsive electrostatic interactions between the counteranion and the ligands negative charges. Thus, although stronger interactions with the metal centers could be achieved by approaching at the less sterically hindered proximities of the μ_3-Q or μ_2-Q ligands, the electron density on these ligands forces the counteranion to approach at different directions and the preferred site is that shown in Figure 3a when the X$^-$ ligand is small (H$^-$, OH$^-$). However, when the size and electron density of X$^-$ increase (Br$^-$), the repulsion with the fluorinated anion becomes more important and forces the counteranion to approach at the direction shown in Figure 3b.

Once the solution structures of the BF$_4^-$ and PF$_6^-$ salts of these trinuclear complexes have been established, it is interesting to make a comparison with the corresponding structures in the solid state. The crystal structures of [W$_3$S$_4$Br$_3$(dmpe)$_3$](PF$_6$) ([**3**]PF$_6$) and [W$_3$Se$_4$Br$_3$(dmpe)$_3$](PF$_6$) ([**6**]-PF$_6$) have been previously reported in the literature,[5,17] and the structures of [W$_3$S$_4$(OH)$_3$(dmpe)$_3$](PF$_6$) ([**2**]PF$_6$) and [W$_3$-Se$_4$H$_3$(dmpe)$_3$](PF$_6$) ([**4**]PF$_6$) have been determined in this work. In this way, the effects of changing the nature of both the chalcogen and the X$^-$ ligand on the interionic solid-state structure can be analyzed. Inspection of the crystal structures of the four PF$_6^-$ salts (see the Supporting Information) reveals interionic interactions similar to those found in CD$_2$-Cl$_2$ solution, but there is no clear tendency in the anion−cation interactions when changing the nature of the chalcogenide or the X$^-$ ligand, which suggests that the solid-state arrangement must be mainly determined by crystal-packing forces.

The Effect of Ion-Pairing on the Kinetics of Reaction of [W$_3$S$_4$H$_3$(dmpe)$_3$]$^+$ with HCl. The findings in the previous section about the structure of cluster−anion ion pairs in dichloromethane solution can be useful in order to rationalize the reactivity of these clusters because it is reasonable to think that the preferred sites of interaction in the ion pairs also represent the most-favorable sites for the
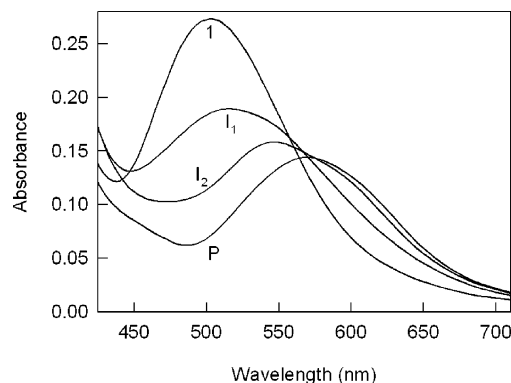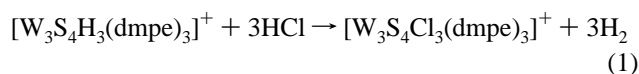
Figure 5. Electronic spectra calculated for the starting complex (**1**), the reaction intermediates ($\mathbf{I_1}$ and $\mathbf{I_2}$), and the final reaction product (**2**) from the spectral changes with time observed during the reaction of cluster 1^+ with HCl in CH$_2$Cl$_2$ solution at 25.0 °C in the presence of 0.05 M Et$_4$-NBF$_4$.

approach of other negatively charged reagents; so, significant differences in reactivity may result from approaches at sites *a* and *b* in Figure 3 in reactions such as the substitution of the X$^-$ ligands. However, the only substitution processes in these clusters whose kinetics has been previously reported[11,12] are the acid-promoted substitutions of coordinated hydrides in 1^+ and 4^+, and these reactions involve the attack by neutral HX molecules. Nevertheless, as these reactions occur through the initial formation of W−H⋯H−X dihydrogen bonds, the formation of ion pairs with fluorine-containing anions interacting with the cluster at the proximities of the coordinated hydrides still anticipates the possible observation of changes in the kinetics of proton transfer from the acid to the hydride. Actually, ion-pairing with BF$_4^-$ has been recently reported to provide an alternative and efficient pathway for the proton transfer from *trans*-[FeH(H$_2$)(dppe)$_2$]$^+$ to a base.[16] For these reasons, the effect caused by the addition of BF$_4^-$ on the kinetics of the acid-promoted substitution of the coordinated hydrides in the 1^+ cluster was studied in CH$_2$Cl$_2$ solution using HCl as the acid (eq 1). Although the complex concentrations used in the kinetic experiments are lower than those in the NMR studies and, consequently, ion-pair formation may be expected to occur at lower extent, the kinetic results clearly evidence changes that can be associated only with the formation of ion pairs.

$$[\text{W}_3\text{S}_4\text{H}_3(\text{dmpe})_3]^+ + 3\text{HCl} \rightarrow [\text{W}_3\text{S}_4\text{Cl}_3(\text{dmpe})_3]^+ + 3\text{H}_2 \tag{1}$$

In the presence of an excess of Et$_4$NBF$_4$, the spectral changes for the reaction in eq 1 are similar to those previously observed for the same reaction in the absence of any added salt[13] and can be fitted by three consecutive exponentials, which yields the rate constants (k_{1obs}, k_{2obs}, and k_{3obs}) and the spectra of the reaction intermediates and the final product included in Figure 5. The calculated spectra are also similar to those derived from experiments in the absence of added salt, for which it was established that the three kinetically resoluble steps correspond to the sequential substitution of the coordinated hydrides by Cl$^-$. The observed rate constants for the three steps show a second-order dependence with respect to the acid concentration (eq 2) that is illustrated in
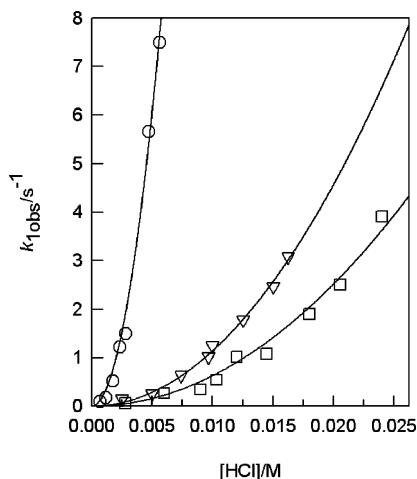
Figure 6. Plots of the observed rate constant vs the acid concentration for the first step in the reaction of $\mathbf{1}^+$ with HCl in CH_2Cl_2 solution at 25.0 °C: (○) in the absence of added Et_4NBF_4; [13] (▽) in the presence of 0.025 M Et_4NBF_4; (□) in the presence of 0.050 M Et_4NBF_4. The solid lines represent the best fit of each set of data to a second-order dependence on the acid concentration.

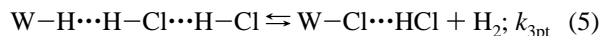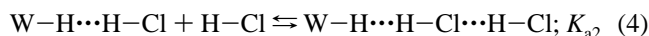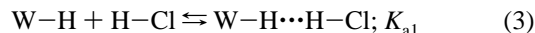**Table 3.** Summary of Kinetic Data for the Reaction of $\mathbf{1}^+$ with HCl in CH_2Cl_2 Solution at 25.0 °C

[Et₄NBF₄] (M)	k_1 (M⁻² s⁻¹)	k_2 (M⁻² s⁻¹)	k_3 (M⁻² s⁻¹)
0[a]	$(2.41 \pm 0.06) \times 10^5$	$(1.03 \pm 0.03) \times 10^4$	[b]
0.025	$(1.14 \pm 0.02) \times 10^4$	$(5.1 \pm 0.1) \times 10^2$	12.8 ± 0.4
0.050	$(6.3 \pm 0.2) \times 10^3$	$(2.9 \pm 0.1) \times 10^2$	7.6 ± 0.2

[a] Data from ref 13. [b] In the absence of added Et_4NBF_4, this rate constant has a value of $(4 \pm 1) \times 10^3$ s⁻¹ and does not show any dependence with the acid concentration.

Figure 6 for the case of k_{1obs}. This figure also shows that addition of Et_4NBF_4 causes a significant decrease in the values of k_{1obs} and that the deceleration becomes more important when the concentration of added salt increases. The numerical values included in Table 3 show that the same effect is observed for k_{2obs} and k_{3obs}, although in the latter case, a direct comparison is not possible because the values derived in the absence of added salt could not be satisfactorily fitted to the rate law in eq 2.[13]
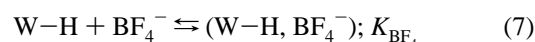
$$k_{iobs} = k_i[HCl]^2 \tag{2}$$

From a combination of experimental and theoretical data, it was previously established that the second-order dependence with respect to the acid results from the formation of dihydrogen-bonded adducts between the $\mathbf{1}^+$ cluster and one or two HCl molecules (eqs 3 and 4).[13] Although both of these adducts may evolve to the final product through two competitive first- and second-order pathways, the adduct with two HCl molecules is favored with respect to that with a single molecule in the presence of an excess of acid; the reaction then goes through the second-order pathway in eq 5. If the equilibria leading to the formation of both adducts are considered to be displaced toward the starting reagents, the rate law for this mechanism (eq 6) coincides with eq 2 with the equivalence $k_1 = k_{3pt}K_{a1}K_{a2}$.

$$W-H + H-Cl \rightleftharpoons W-H\cdots H-Cl; K_{a1} \tag{3}$$

$$W-H\cdots H-Cl + H-Cl \rightleftharpoons W-H\cdots H-Cl\cdots H-Cl; K_{a2} \tag{4}$$

$$W-H\cdots H-Cl\cdots H-Cl \rightleftharpoons W-Cl\cdots HCl + H_2; k_{3pt} \tag{5}$$

$$k_{obs} = k_{3pt}K_{a1}K_{a2}[HCl]^2 \tag{6}$$

The kinetic data obtained in the presence of added BF_4^- can be easily interpreted by including in this mechanism the formation of ion pairs between $\mathbf{1}^+$ and the anion (eq 7). If these ion pairs do not lead to product formation, the rate law is given by eq 8; the presence of added BF_4^- is expected to cause a decrease in the reaction rate by a factor of $1:(1 + K_{BF4}[BF_4^-])$. In agreement with this expectation, a consistent value of $K_{BF4} = (7.8 \pm 0.4) \times 10^2$ M⁻¹ is obtained from the decrease in the k_1 values at two different concentrations of this anion. Although a quite close value of $(7.3 \pm 0.6) \times 10^2$ M⁻¹ can be obtained from the k_2 decrease, this value corresponds to the equilibrium constant for the formation of an ion pair between BF_4^- and $[W_3S_4H_2Cl(dmpe)_3]^+$. The similarity between both values indicates that substitution of one H⁻ by Cl⁻ does not significantly change the stability of the ion pair. Unfortunately, no estimation of K_{BF4} can be made from the k_3 values because of the different units of the rate constant derived in the absence of added salt. Although the description of the system in terms of one-to-one ion pairing, as represented in eq 7, is probably a simplification and other anions may also interact simultaneously with the cluster cation, these last aggregates are expected to be less stable on the basis of electrostatic and steric grounds. The excellent agreement calculated by considering ion pairs with only one BF_4^- anion indicates that ion pairs involving more anions, if they exist, are in much lower concentrations.

$$W-H + BF_4^- \rightleftharpoons (W-H, BF_4^-); K_{BF_4} \tag{7}$$

$$k_{obs} = \frac{k_{3pt}K_{a1}K_{a2}[HCl]^2}{1 + K_{BF_4}[BF_4^-]} \tag{8}$$

Theoretical Studies on the Effect of Ion Pairing on the Mechanism of Proton Transfer to the Coordinated Hydride. The experimental results in the previous sections indicate that BF_4^- forms an ion pair with $\mathbf{1}^+$ where the anion is placed close to the coordinated hydrides, which causes a deceleration of the proton-transfer process from HCl that can be intuitively understood invoking steric reasons. However, it has been previously reported that ion-pairing with BF_4^- increases the rate of deprotonation of dihydrogen complex *trans*-$[FeH(H_2)(dppe)_2]^+$.[16] Although in that case the reaction was monitored in the reverse direction, microscopic reversibility dictates that the formation of ion pairs with this anion must also result in an increase in the rate of proton transfer to the coordinated hydride. However, the results in the present work for the reaction of $\mathbf{1}^+$ with HCl indicate just the opposite effect, so that the deceleration observed upon the addition of BF_4^- reveals that ion-pairing does not in this case provide an alternative efficient pathway for proton

Table 4. Summary of Energies Calculated for the Different Species Resulting from the Interaction of the Model Cluster $1m^+$ with BF_4^- and HCl^a

| | gas phase | dicholoromethane solution | |
species	ΔE (kcal mol^{-1})	ΔE (kcal mol^{-1})	ΔG (kcal mol^{-1})
$1m^+$–HCl Adducts^b			
W–H···H–Cl	−3.06	−2.90	−0.76
W–H···H–Cl···H–Cl	−9.21	−7.74	−3.78
HCl–BF_4^- Adducts			
Cl–H···BF_4^-	−16.85	−7.16	−6.29
Cl–H···Cl–H···BF_4^-	−26.76	−11.37	−9.59
Cl–H···BF_4^-···H–Cl	−30.75	−14.60	−12.68
$1m^+$–HCl–BF_4^- Adducts			
$(1m^+, BF_4^-)$	−65.80	−6.37	−4.04
$(1m^+, 2BF_4^-)$	−90.00	−10.27	−6.08
2t	−79.66	−15.64	−11.40
3t	−78.37	−15.76	−10.60
4t	−73.31	−11.72	−5.82
5t	−86.71	−21.04	−14.17
6t	−88.38	−21.52	−14.98
7t	−91.16	−24.55	−18.37
8t	−80.13	−17.51	−9.93
9t	−79.51	−15.77	−6.94
10t	−86.83	−21.35	−11.37

^{a} All the values are given relative to the separated species. ^{b} Data from ref 13.

transfer, as observed for the Fe complex. In an attempt to understand the reasons that lead to such a different behavior in both complexes, theoretical studies were carried out using model cluster $[W_3S_4H_3(PH_3)_6]^+$ ($1m^+$), which has been previously revealed to be very useful for understanding the rate law and mechanism of the reaction of the cluster with HCl.[13] Although the HOESY spectra indicate the location of the fluorinated anion at the proximities of the methyl groups of the cluster and inclusion of these groups in the calculations would be desirable, attempts to make calculations with a model including the dmpe ligands are extremely slow with the computer power available even for the isolated cluster, which precludes calculations on the interaction with the anion and the acid. Despite the limitations of the simplified model, clarifying results could still be obtained. As the DFT calculations carried out involve the formation of adducts that contain a variable number of species, the entropy contributions can be specially important; thus, the discussion in the next paragraphs is on the basis of the free energies calculated for each adduct in dichloromethane solution. However, Table 4 also includes the corresponding values of the potential energies in both the gas phase and CH_2Cl_2 solution, facilitating comparison with the values reported for related systems. The Cartesian coordinates corresponding to the different adducts discussed in the text are given in the Supporting Information.

The interaction between $1m^+$ and BF_4^- leads to the formation of a $(1m^+, BF_4^-)$ ion pair stabilized by 4.04 kcal mol^{-1} in CH_2Cl_2 solution whose optimized geometry (Figure 7) shows the anion at the proximities of the coordinated hydride with three short H–F distances of 2.67, 2.98, and 3.19 Å. This structure agrees with the NMR results, although the presence of the methyl groups probably makes the distances somewhat larger in the real system, as revealed by the absence of W–H···F signals in the HOESY spectrum. Actually, significant interactions between the F atoms of

BF_4^- and the hydrogens of PH_3 are observed in the model used (shortest F···H distances of 1.93 and 1.97 Å), and they surely contribute to the docking of the BF_4^- anion. When a second BF_4^- is added to the model, the calculations reveal the formation of a new $(1m^+, 2BF_4^-)$ species with an optimized geometry (Figure 7) that shows each BF_4^- anion close to a different W–H bond. However, the stabilization achieved with the second anion (2.04 kcal mol^{-1} in CH_2Cl_2) is significantly lower than that with the first one. For this reason and because the experimental kinetic data show a clear dependence on the BF_4^- concentration without evidence of higher-order contributions, a single anion was included in the ion pair model used to theoretically investigate potential interactions with HCl molecules.

Once the structure of the $(1m^+, BF_4^-)$ ion pair had been established, the geometries and energies of the adducts resulting from the interaction of this ion pair with one and two HCl molecules were calculated to make a comparison with the corresponding adducts in the absence of BF_4^-. The inclusion of one HCl molecule in the calculations leads to the formation of stable $(1m^+, BF_4^-, HCl)$ adducts, for which the optimized geometries resulting from HCl approach at different sites were calculated (see Figure 7). The results indicate that there are two almost degenerate structures (**2t** and **3t**) in which the HCl molecule approaches the ion pair at the proximities of the BF_4^- anion. The most stable of these structures (**2t**) is stabilized by 7.36 kcal mol^{-1} with respect to the $(1m^+, BF_4^-)$ ion pair, with the HCl molecule located close to both ions. The optimized geometry shows a H···H distance (2.68 Å) too large to be considered a dihydrogen bond and hence **2t** must be considered unproductive for proton transfer.

Actually, in the absence of BF_4^-, the calculations revealed the formation of a W–H···H–Cl adduct with a much stronger H···H interaction (d_{H-H}= 1.36 Å)[13] that facilitates the release of H_2 in the next step. In the alternative **3t** structure, which is only 0.80 kcal mol^{-1} less stable than **2t**, the HCl molecule interacts with BF_4^-; there is no W–H···HCl interaction, which makes this adduct unproductive for proton transfer as well. The stabilization observed for both **2t** and **3t** can be attributed to the interaction of HCl with the anion and, as a matter of fact, theoretical calculations reveal the formation of cluster-free ClH···BF_4^- adducts stabilized by 6.29 kcal mol^{-1} in CH_2Cl_2 solution. This indicates that most of the stabilization achieved in the **2t** and **3t** adducts can be considered to come from an additive interaction of BF_4^- with both the cluster and the acid. It is also important to note that the stability of ClH···BF_4^- implies the formation of significant amounts of this species in dichloromethane solution, causing a decrease in the effective HCl concentration and the subsequent deceleration of the proton-transfer process; BF_4^- acts as a scavenger for the HCl molecules.

Although our theoretical results just discussed clearly indicate that ion-pairing with BF_4^- hinders the formation of HCl adducts capable of undergoing proton transfer, the validity of this conclusion is limited to adducts in which HCl approaches the W–H bond close to the BF_4^- anion.
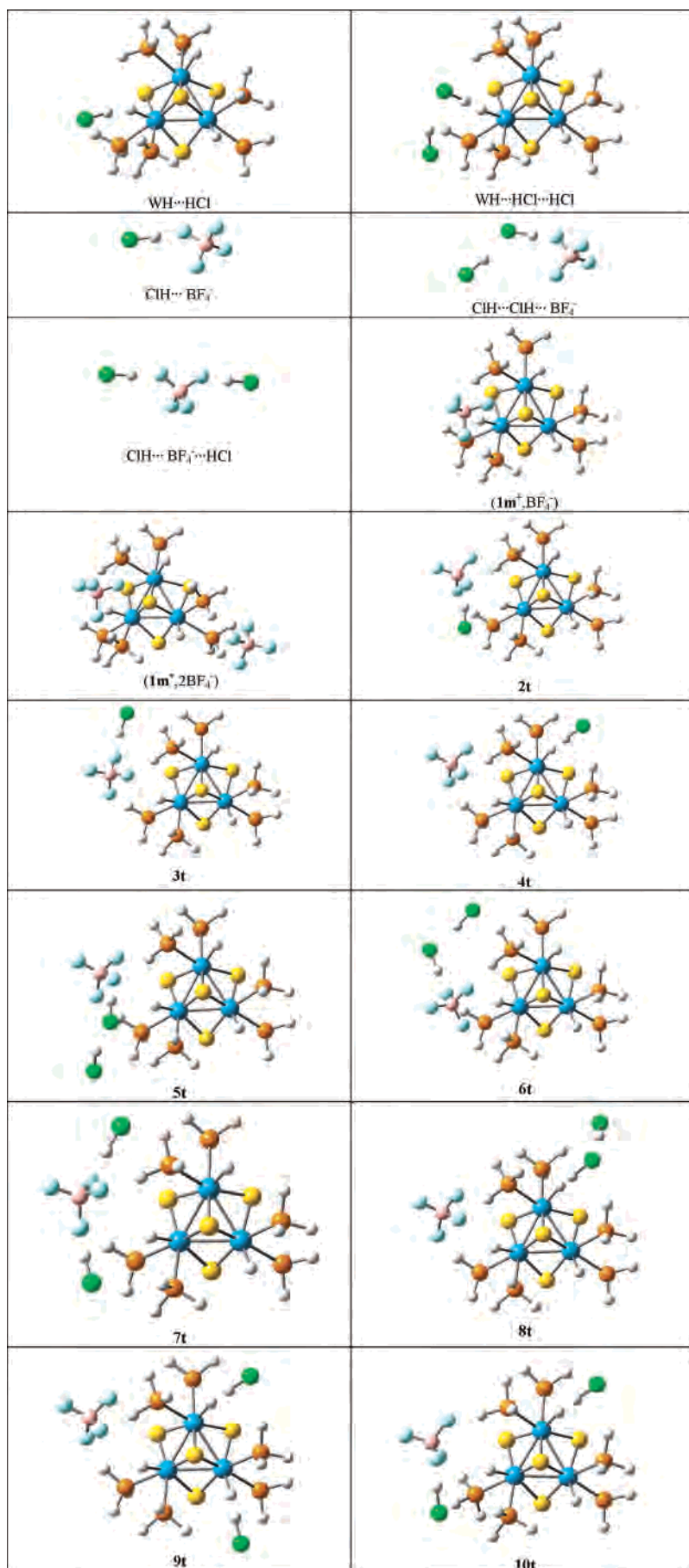
Figure 7. Optimized geometries for the different species resulting from the interaction of model cluster **1m**⁺ with BF₄⁻ and HCl.

However, the possibility that HCl approaches the cluster at one of the other W−H bonds cannot be ruled out. The optimized geometry obtained for the corresponding adduct, **4t** in Figure 7, shows a W−H···H−Cl dihydrogen bond with a H···H distance (1.17 Å) that is shorter than that found for the corresponding adduct in the absence of BF_4^- (1.36 Å); consequently, **4t** can evolve into the reaction products. However, **4t** is significantly less stable than **2t** (5.58 kcal mol^{-1} in CH_2Cl_2 solution; the interaction of one HCl molecule with the (**1m**$^+$, BF_4^-) ion pair would occur preferentially at the unproductive W−H site, thus justifying the deceleration of the proton-transfer process.

The results obtained when a second HCl molecule is added to the theoretical model lead to conclusions similar to those derived from calculations with a single molecule of acid. When the second HCl approaches the **2t** and **3t** adducts at the proximities of the previously existing HCl molecule, two almost degenerate adducts (**5t** and **6t**, see optimized geometries in Figure 7) arise, both of them containing a hydrogen bond between the HCl molecules and being ca. 3.5 kcal mol^{-1} more stable than the corresponding adducts with a single HCl. However, as seen for **3t**, the molecules of acid in **6t** are placed too far away from the coordinated hydride to allow proton transfer. Analogously to **2t**, the proton− hydride distance in the W−H···HCl···HCl arrangement of **5t** is too large (2.92 Å) to consider it a dihydrogen bond; this adduct is unproductive for the proton-transfer process as well. Moreover, the most-stable adduct resulting from the interaction of (**1m**$^+$, BF_4^-) with two HCl molecules does not show a HCl···HCl hydrogen bond. Instead, the acid molecules in the optimized structure (**7t** in Figure 7) approach different F atoms of the BF_4^- anion, so that **7t** can be described as the result of the interaction of the cluster with a ClH···BF_4^-···HCl unit. Adduct **7t** is 3.39 kcal mol^{-1} more stable than **6t** in CH_2Cl_2 solution, but the shortest proton− hydride distance is again too large (3.16 Å) and makes this adduct unproductive. In addition, cluster-free ClH···BF_4^-···HCl and ClH···ClH···BF_4^- aggregates are found to be quite stable in CH_2Cl_2 solution, with stabilization energies of 12.68 and 9.59 kcal mol^{-1}, respectively. The formation of significant amounts of these species under the conditions of the kinetic experiments can be again invoked to explain, at least in part, the observed deceleration.

Theoretical calculations were also carried out considering that the second HCl molecule approaches the cluster at the proximities of metal centers far from the BF_4^- anion. In this way, adducts **8t**−**10t** were obtained, whose optimized geometries are also shown in Figure 7. Although all of these adducts contain W−H···HCl dihydrogen bonds with H···H distances of 0.96 Å (**8t**), 1.18 and 1.23 Å (**9t**), and 1.19 Å (**10t**) that make possible the subsequent release of H$_2$, they are expected to be formed at low concentrations because of their lower stability with respect to **7t** (**8t**, **9t**, and **10t** are 8.44, 11.43, and 7.00 kcal mol^{-1} less stable than **7t**, respectively). Actually, the stabilization achieved in the **8t**− **10t** adducts through the interaction of one **1m**$^+$ ion with one BF_4^- and two HCl molecules is lower than that achieved in the cluster-free ClH···BF_4^-···HCl adduct.
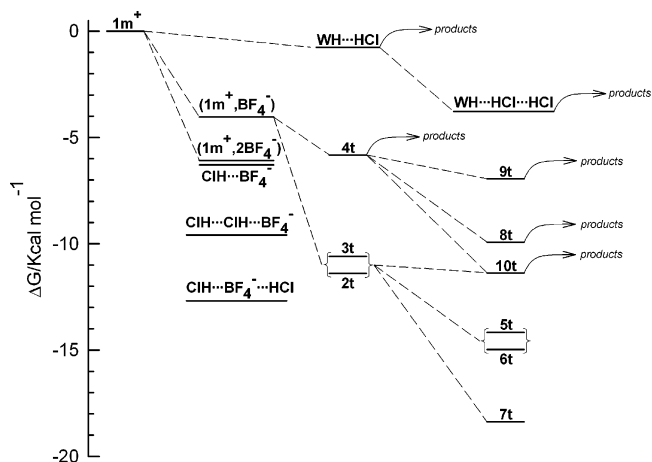
Figure 8. Relative free energies calculated in CH_2Cl_2 solution for the HCl adducts formed by the free **1m**$^+$ cluster, the BF_4^- anion, and the (**1m**$^+$, BF_4^-) ion pair.

Figure 8 summarizes the results of the theoretical calculations on the formation of adducts between **1m**$^+$ and one or two HCl molecules in both the absence and presence of BF_4^-. Ion-pairing to BF_4^- leads in all cases to stabilization, but it is important to note that the most-stable HCl adducts are unproductive for proton transfer. In any case, the variety of adducts possible leads to the conclusion that the mechanism of proton transfer from HCl to cluster **1** in the presence of added BF_4^- can be more complex than that depicted in eqs 3−5 and 7. From the distribution of energies in Figure 8, a mixture of adducts must be reasonably expected to be formed in solution, and this allows for a variety of reaction pathways too complex to be analyzed in detail. However, one important conclusion is that BF_4^- interacts with both reagents (the cluster and HCl) to form quite stable (**1**, BF_4^-), ClH···BF_4^-, ClH···ClH···BF_4^-, and ClH···BF_4^-···HCl adducts that reduce the concentrations of the free reagents in solution and cause a deceleration of the proton transfer through the pathway operating in the absence of BF_4^-. In addition, although the (**1**, BF_4^-) ion pairs can form several types of adducts with HCl, the most stable of these adducts will represent dead-ends in the mechanism because they do not contain the W−H···HCl dihydrogen bonds required to complete the proton transfer. The only BF_4^--containing adducts capable of evolving into the reaction products are those in which at least one HCl molecule forms a dihydrogen bond with one of the W−H centers far from the BF_4^- anion, but the contribution of possible pathways involving these adducts will not be important because they are significantly less stable than other adducts and actually, their formation is less favored than that of the cluster-free ClH···BF_4^-···HCl adduct.

At this point, it is interesting to compare the effect of ion-pairing on proton-transfer processes in our cluster hydride and other related mononuclear hydride complexes. In our case, the reaction goes through the formation of dihydrogen-bonded adducts, where the simultaneous interaction of BF_4^- (and related anions) with both the metal hydride and the proton donor leads to adducts lacking of dihydrogen bonds or with H···H distances larger than those observed in the

absence of ion-pairing. This effect causes a decrease in the proton-transfer reaction rate and contrasts with recent reports showing that ion-pairing can even result in a shortening of the H−H distance in dihydrogen mononuclear complexes (1.05 Å for free $[Cp^*OsH_4(PPh_3)]^+$ and 0.94 Å for its adduct with BF_4^-; 1.35 Å for free $[Os(H_2)Cl(dppe)_2]^+$ and 1.11 Å for its ion pair with PF_6^-, 0.855 Å for $[NbCp_2(H_2)_2]^+$ and 0.836 Å for its ion pair with $H(TFA)_2^-$, TFA = trifluoroacetate).[21−23] However, these complexes differ from the dihydrogen-bonded adducts WH···HCl reported in this work, because the H−H bond of stable mononuclear dihydrogen complexes cannot be broken as a consequence of weak interactions with the anion. Nevertheless, these interactions can lead to relatively small changes in the H−H distances that, at least for the quoted examples, appears to be favored in the sense of a shortening the H−H bond. In contrast, the hydrogen atoms involved in a dihydrogen bond are only weakly bound to each other, and the H···H distance can undergo more-pronounced changes upon interaction with an external anion. For the case of BF_4^- and other fluorinated anions interacting with an M−H···H−X dihydrogen-bonded adduct, the F_3-BF^-···H−X interactions will reduce the capability of the acid to participate in dihydrogen bonding, which can lead to quite large increases in the H···H distance. The extreme case would be that represented by structures such as **3t** or **6t**, in which the fluorinated anion inserts between M−H and H−X and causes the complete breaking of the dihydrogen bond, thus blocking this reaction pathway. However, there is also the possibility that BF_4^- interacts with the M−H···H−X dihydrogen-bonded adduct to form a stable ternary species without largely perturbing the H···H distance. This is the case of the reaction of *trans*-$[FeH(H_2)(dppe)_2]^+$ with NMe_3, for which the calculations revealed that the interaction with BF_4^- leads to only a minor change, from 1.211 to 1.283 Å, in the H···H distance of the dihydrogen-bonded intermediate; the BF_4^- follows the proton along its transfer, and the additional stabilization achieved through the formation of stable $(HNMe_3^+, BF_4^-)$ ion pairs as reaction products leads to an acceleration of the proton-transfer process.[16]

Conclusion

NMR techniques have been used to demonstrate the formation of ion pairs between the $[W_3Q_4X_3(dmpe)_3]^+$ (Q= S, Se; X= H, OH, Br) cationic clusters and the BF_4^- and PF_6^- anions in dichloromethane solutions. These ion pairs have well-defined structures that depend on the nature of both the cluster and the external anion, and although the interactions within these ion pairs are significantly weaker than covalent bonds, experimental and theoretical evidences accumulated in recent times clearly indicate that this kind of species cannot be ignored when a precise understanding of the reactivity of the complexes is desired. The ($[W_3S_4H_3$-

$(dmpe)_3]^+$, BF_4^-) ion pair, with a structure in which BF_4^- approaches the cluster at the proximities of one of the coordinated hydrides, constitutes an excellent example of reactivity changes due to ion pairing. In this case, the kinetics and mechanism of proton transfer from an acid (HCl) to the coordinated hydride is largely affected for several reasons. First, the formation of ($\mathbf{1}^+$, BF_4^-), ClH···BF_4^-, ClH···Cl-H···BF_4^-, and ClH···BF_4^-···HCl reduce the concentrations of $\mathbf{1}^+$ and BF_4^- and make the reaction slower through the formation of BF_4^--free HCl adducts of $\mathbf{1}^+$. Second, although ($\mathbf{1}^+$, BF_4^-) can still interact with the HCl molecules approaching at the proximities of BF_4^-, the resulting adducts lack W−H···HCl dihydrogen bonds and are thus unable to undergo proton transfer. Third, the interaction of HCl with the other two W−H bonds opposite to the BF_4^- anion leads to dihydrogen-bonded species capable of providing efficient pathways for proton transfer; however, the lower stability of these adducts reduces the contribution of potential pathways involving these species to the net rate of the reaction.

Experimental Section

Synthesis and Physical Measurements. The PF_6^- salts of the molecular triangular clusters $\mathbf{1}^+$−$\mathbf{6}^+$, $[W_3Q_4X_3(dmpe)_3](PF_6)$, were prepared according to literature methods.[11,12,17,19,24] The corresponding tetrafluoroborate salts were prepared by the same procedure but using acetone solutions of $NaBF_4$ instead of KPF_6 during the chromatographic work up. The purity of the samples was confirmed by electrospray mass spectra (recorded on a Micromass Quattro LC instrument using nitrogen as the drying and nebulizing gas and CH_2Cl_2 as the solvent).

The $^{31}P\{^1H\}$, NOESY1D, and ^1H NMR spectra were obtained using CD_2Cl_2 solutions of the complexes (ca. 0.01 mol dm⁻³) with a Varian Inova 400 spectrometer, using the standard pulse sequences provided by the manufacturer. The $^1H,^{19}F$ HOESY experiments were recorded with the same instrument using the hoesy_da pulse sequence with a mixing time of 0.4 s.

X-ray Data Collection and Structure Refinement. Crystals suitable for X-ray studies of the PF_6^- salts of clusters $\mathbf{2}^+$ and $\mathbf{4}^+$ were grown by slow diffusion of ether into CH_2Cl_2 solutions. The crystals are air-stable and were mounted on the tip of a glass fiber with the use of epoxi cement. X-ray diffraction experiments were carried out at room temperature with a Bruker SMART CCD diffractometer using Mo Kα radiation (λ = 0.71073 Å). The data were collected with a frame width of 0.3° in ω and a counting time of 20 s per frame. The diffraction frames were integrated using the SAINT package and corrected for absorption with SADABS.[25,26] The structures were solved by direct methods and refined by the full-matrix method on the basis of F^2 using the SHELXTL software package.[27]

Crystal Structure of [2](PF₆). The structure was successfully solved in space group $I23$ considering a merohedral racemic twinning with final BASF (batch scale factor) values of 0.50(4). All the non-hydrogen atoms within the cluster except carbons were refined anisotropically, whereas the positions of the hydrogen atoms

(21) Webster, C. E.; Gross, C. L.; Young, D. M.; Girolami, G. S.; Schultz, A. J.; Hall, M. B.; Eckert, J. *J. Am. Chem. Soc.* **2005**, *127*, 15091.

(22) Gusev, D. G. *J. Am. Chem. Soc.* **2004**, *126*, 14249.

(23) Bakhmutova, E. V.; Bakhmutov, V. I.; Belkova, N. V.; Besora, M.; Epstein, L. M.; Lledós, A.; Nikonov, G. I.; Shubina, E. S.; Tomàs, J.; Vorontsov, E. V. *Chem.−Eur. J.* **2004**, *10*, 661.

(24) Estevan, F.; Feliz, M.; Llusar, R.; Mata, J. A.; Uriel, S. *Polyhedron* **2001**, *20*, 527.

(25) *SAINT*; Bruker Analytical X-ray Systems: Madison, WI, 2001.

(26) Sheldrick, G. M. *SADABS Empirical Absorption Program*; University of Göttingen: Göttingen, Germany, 2001.

(27) Sheldrick, G. M. *SHELXTL*; Brucker Analytical X-ray Systems: Madison, WI, 1997.

were generated geometrically, assigned isotropic thermal parameters, and allowed to ride on their respective parent carbon atoms. One of the PF_6^- anion lies on a special position (intersection of three 2-fold axis), and its atoms were also refined anisotropically. This accounts for six out of the eight negative charges within the unit cell. The other set of independent PF_6^- ions revealed in the Fourier map as highly disordered were refined as a rigid group with perfect octahedral geometry, placing the phosphorus atom on the highest electron density peak.

The site occupancies of the highly disordered PF_6^- anions were assigned to ensure a cluster:PF_6^- ratio of 1, compatible with the observed cluster charge. The refinement gives three PF_6^- congeners around a 3-fold axis that filled part of the existing structure hole. This kind of disorder is often observed in $[M_3M'Q_4(dmpe)_3X_3][PF_6]$ complexes that crystallize in the cubic space group $I23$.[8,17] Empirical formula $C_{18}H_{51}O_3F_6P_7S_4W_3$; FW = 1326.17; crystal system cubic; unit cell dimensions $a = 20.739(2)$ Å; volume = 8919.3(15) Å^3; T = 293(2) K; space group $I23$; $Z = 8$; $\mu = 8.202$ mm^{-1}; no. of reflections collected = 20 195; no. of independent reflections = 1956 [R(int) = 0.0437]; Final R indices [$I > 2\sigma(I)$] R1 = 0.0497, wR2 = 0.1297; R indices (all data) R1 = 0.0500, wR2 = 0.1301. The highest residual electron density was 3.1 e/Å^3, near the tungsten atoms

Crystal Structure of [4](PF$_6$). The structure was successfully solved in the monoclinic space group $C2/c$. All the non-hydrogen atoms except the fluorine atoms in the PF_6^- ion were refined anisotropically. The positions of the hydrogen atoms were generated geometrically, assigned isotropic thermal parameters, and allowed to ride on their respective parent carbon atoms. Two independent PF_6^- anions with the phosphorus atoms both in the special position 4e were found in the structure. The last Fourier map showed one-half a molecule of dichloromethane.

Empirical formula $C_{18.50}H_{52}ClF_6P_7Se_4W_3$; FW = 1508.23; crystal system monoclinic; unit cell dimensions $a = 25.750(7)$ Å, $b = 21.090(6)$ Å, $c = 16.839(5)$ Å, $\beta= 111.056(6)°$: volume = 7425-(3) Å^3; $T = 293(2)$ K; space group $C2/c$; $Z = 8$; $\mu = 11.843$ mm^{-1}; no. of reflections collected = 19 341; no. of independent reflections = 5580 [R(int) = 0.1890]; Final R indices [$I > 2\sigma(I)$] R1 = 0.0784, wR2 = 0.1555; R indices (all data) R1 = 0.1680, wR2 = 0.1986.

Kinetic Experiments. The kinetic experiments were carried out at 25.0 °C using an Applied Photophysics SX17MV stopped-flow instrument provided with a PDA.1 diode-array detector, and the results were analyzed with the SPECFIT program.[28] The complex ([**1**]PF$_6$) solutions contained the amount of Et$_4$NBF$_4$ required to keep a constant ionic strength, at the concentrations indicated in the previous section, in the resulting solutions. Reaction of ClSiMe$_3$ with MeOH was used to obtain HCl in neat CH$_2$Cl$_2$. The concentration of acid was determined in each case by titration with a previously standardized KOH solution. These titrations were carried out after diluting an aliquot (1−2 mL) with water (50 mL). All kinetic experiments were carried out under pseudo-first-order conditions of acid excess, the concentrations of the cluster being within the range (0.6−5.2) × 10^{-4}M.

Theoretical Calculations. The theoretical study has been conducted with the Becke hybrid density functional (B3LYP)[29] method as implemented in the Gaussian98 program.[30] The double-ζ pseudo-orbital basis set LanL2DZ, in which W, S, and P atoms are represented by the relativistic core LanL2 potential of Los Alamos,[31] was used. Solvent effects were taken into account by means of polarized continuum model calculations[32] using standard options. The energies of solvation were computed in dichloromethane ($\epsilon = 8.93$) at the geometries optimized in the gas phase.

Supporting Information Available: Comments, with figures, on the assignment of the signals in the proton and phosphorus NMR spectra of the $[W_3Q_4X_3(dmpe)_3]^+$ clusters and the crystal structure of $[W_3Q_4X_3(dmpe)_3](PF_6)$ complexes; X-ray crystallographic files in CIF format for compounds [**2**]PF$_6$ and [**4**]PF$_6$; Cartesian coordinates of the theoretically calculated structures. This material is available free of charge via the Internet at http://pubs.acs.org.

IC0520770

(28) Binstead, R. A.; Jung, B.; Zuberbühler, A. D. *SPECFIT-32*; Spectrum Software Associates: Chappel Hill, NC, 2000.

(29) (a) Lee, C.; Yang, Y.; Parr, R. G. *Phys. Rev. B: Condens. Matter Mater. Phys.* **1988**, *37*, 785. (b) Becke, A. D. *J. Chem. Phys.* **1993**, *98*, 5648.

(30) Frisch, M. J.; Trucks, G. W.; Schlegel, H. B.; Scuseria, G. E.; Robb, M. A.; Cheeseman, J. R.; Zakrzewski, V. G.; Montgomery, J. A., Jr.; Stratmann, R. E.; Burant, J. C.; Dapprich, S.; Millam, J. M.; Daniels, A. D.; Kudin, K. N.; Strain, M. C.; Farkas, O.; Tomasi, J.; Barone, V.; Cossi, M.; Cammi, R.; Mennucci, B.; Pomelli, C.; Adamo, C.; Clifford, S.; Ochterski, J.; Petersson, G. A.; Ayala, P. Y.; Cui, Q.; Morokuma, K.; Malick, D. K.; Rabuck, A. D.; Raghavachari, K.; Foresman, J. B.; Cioslowski, J.; Ortiz, J. V.; Baboul, A. G.; Stefanov, B. B.; Liu, G.; Liashenko, A.; Piskorz, P.; Komaromi, I.; Gomperts, R.; Martin, R. L.; Fox, D. J.; Keith, T.; Al-Laham, M. A.; Peng, C. Y.; Nanayakkara, A.; Gonzalez, C.; Challacombe, M.; Gill, P. M. W.; Johnson, B.; Chen, W.; Wong, M. W.; Andres, J. L.; Gonzalez, C.; Gordon, M.; Replogle, E. S.; Pople, J. A. *Gaussian 98*; Pittsburgh, PA, 1998.

(31) Hay, P. J.; Wadt, R. *J. Chem. Phys.* **1985**, *82*, 270.

(32) (a) Tomasi, J.; Persico, M. *Chem. Rev.* **1994**, *94*, 2027. (b) Amovilli, C.; Barone, V.; Cammi, R.; Cancès, E.; Cossi, M.; Menucci, B.; Pomelli, C. S.; Tomasi, J. *Adv. Quantum Chem.* **1998**, *32*, 227.